acetonitrile are −0.12 and −1.24 V vs. $Cp_2Fe^{+/0}$, respectively.

Table IV summarizes the formal potentials and reactivity toward the oxidation of alcohols of a series of ruthenium–TMC complexes in various oxidation states. One generalization that emerges from these data is that the monooxo complexes of Ru(V) are the most active catalysts with the ligand trans to the oxo ligand exerting a very strong effect on the reactivity.

The fact that the rates of the catalyzed oxidations of alcohols do not respond simply to changes in the oxidizing strength of the catalyst argues against an outer-sphere mechanism for the catalyzed reaction. Since reaction 4 involves the transfer of both a proton and an electron (or a hydrogen atom) from the alcohol, it is tempting to regard the oxo ligand as facilitating the transfers by helping to stabilize the departing proton. The ability of the oxo ligand to function in this way could well be strongly influenced by the nature of the other trans ligand, with saturated ligands such as chloride being preferable to ligands such as oxo or azido because of potential $p\pi$(ligand)–$d\pi^*$(Ru)–$p\pi$(O) interactions. This would provide a rationalization for reactivities that do not correlate simply with the formal potentials of the catalysts.

The chemistry of mononuclear Ru(V)–oxo complexes is relatively unexplored,[15] and studies with a greater variety of trans ligands will be necessary to provide less speculative interpretations of the catalytic reactivity patterns that have been encountered.

Acknowledgment. This work was supported by the U.S. National Science Foundation (Caltech) and the Committee on Conference and Research grants of the University of Hong Kong.

(15) See, for example: Seddon, E. A.; Seddon, K. R. In *The Chemistry of Ruthenium*; R. J. H., Clark, Ed.; Elsevier: Amsterdam, 1984; Chapter 6.

Contribution from the Departments of Chemistry, McMaster University, Hamilton, Ontario L8S 4M1, Canada, and University of Toronto, Toronto, Ontario M5S 1A1, Canada

Dilead(II) Chalcogenide Anions $Pb_2Ch_3^{2-}$ (Ch = Se, Te): A ^{207}Pb, ^{125}Te, and ^{77}Se Solution NMR Study. X-ray Crystal Structure of (2,2,2-crypt-K^+)$_2Pb_2Se_3^{2-}$

Mår Björgvinsson,[†] Jeffery F. Sawyer,[‡] and Gary J. Schrobilgen*[†]

Received June 16, 1986

A new series of dilead(II) chalcogenide anions, $Pb_2Ch_3^{2-}$ (Ch = Se, Te), has been obtained by extraction of the appropriate ternary or quaternary Zintl phases of the type $KPb_xSe_{(3-n)/3}Te_{n/3}$ (where $x \approx {}^1/_2$ and n = 0–3) with ethylenediamine (en) in the presence of 2,2,2-crypt and have been characterized in en solution by ^{207}Pb, ^{125}Te, and ^{77}Se NMR spectroscopy. The coupling constants $^1J_{^{207}Pb-^{125}Te}$ and $^1J_{^{207}Pb-^{77}Se}$ have been determined for all four possible anions, $Pb_2Se_xTe_{3-x}^{2-}$ (x = 0–3), enabling structural comparisons within the series after the nuclear dependence has been removed to give reduced coupling constants $^1K_{Pb-Te}$ and $^1K_{Pb-Se}$. Allowances have also been made for relativistic effects, which are of major importance in heavy-element spin–spin coupling and in the series of anions under consideration. The NMR findings indicate that the structures of the anions are based upon a trigonal bipyramid having axial lead atoms bonded to three chalcogen atoms in the equatorial plane and are supported by the X-ray crystal structure of (2,2,2-crypt-K^+)$_2Pb_2Se_3^{2-}$, which has been determined at room temperature. This compound crystallizes in the monoclinic system, space group $P2_1/n$, with four molecules in a unit cell of dimensions a = 10.320 (4) Å, b = 47.011 (11) Å, c = 11.430 (4) Å, and β = 90.25 (4)°, with R = 0.1184 for 3956 observed ($I > 3\sigma(I)$) reflections. In addition to eight 2,2,2-crypt-K^+ cations, the structure also contains four trigonal-bipyramidal $Pb_2Se_3^{2-}$ anions per unit cell with essentially D_{3h} symmetry. The Pb–Se distances are 2.726 (5)–2.792 (8) Å with Pb–Se–Pb angles of 70.4 (1)–70.9 (1)° and Se–Pb–Se angles of 87.1 (2)–91.6 (1)°. The distance between the two axial lead atoms is only 3.184 (3) Å and is substantially less than the accepted van der Waals contact.

Introduction

Although much of the earlier work on Zintl anions has produced cluster, cage, or ring cluster species, numerous examples of heteroatomic classically bonded anions extracted from Zintl alloys have come to light. (For an excellent recent review of these topics, see ref 1). It is apparent in the recent literature that extraction of Zintl alloys of mixtures of electropositive elements such as Hg, Tl, Sn, with As and electronegative elements such as Se and Te in ethylenediamine produces classical anions, e.g., $HgTe_2^{2-}$,[2] $SnTe_4^{4-}$,[3] and $As_2Se_6^{2-}$.[4] There also exist a number of solid-state structural findings on Zintl phases that contain classically bonded anions prepared by conventional means other than Corbett's alloy extraction technique (vide infra). The bulk of this work has been summarized in two recent reviews.[5]

In the most recent studies in our laboratory, the extraction of Zintl phases in ethylenediamine (en) or liquid ammonia in the presence of 2,2,2-crypt (4,7,13,16,21,24-hexaoxa-1,10-diazabicyclo[8.8.8]hexacosane) has given rise to solutions containing $HgCh_2^{2-}$, $SnCh_3^{2-}$, $TlCh_3^{3-}$, $SnCh_4^{4-}$, and $Tl_2Ch_2^{2-}$, where Ch = Se, Te.[6] The octadentate alkali-metal-ion sequestering agent 2,2,2-crypt has been used by Corbett and his co-workers to prevent reversion of the Zintl species to their respective intermetallic phases upon isolation from the solvent medium and, in a number of instances, has led to the formation of crystalline material suitable for X-ray structure analyses. In our studies, the cryptand also serves to greatly enhance the rate of solution extraction of the alkali-metal alloy and the solubility of the anion species. The latter factor is of critical practical importance to the investigation of these ordinarily dilute solutions by NMR spectroscopy. Consequently, all of the aforementioned species have been characterized in solution by direct NMR observation of the naturally abundant and/or enriched spin-$^1/_2$ isotopes $^{203,205}Tl$, ^{199}Hg, ^{119}Sn, ^{77}Se, and ^{125}Te. Multinuclear magnetic resonance spectroscopy has proven to be well-suited to the rapid and representative characterization of the chemistry of solution extracts of Zintl anions by virtue of the fact that every post-transition-metal element capable of forming a Zintl phase possesses at least one naturally abundant NMR-active isotope, which, by virtue of its nonquadrupole nature, can provide additional valuable structural information based upon its hetero- or homonuclear spin–spin couplings.

[†] McMaster University.
[‡] University of Toronto.

(1) Corbett, J. D. *Chem. Rev.* **1985**, *85*, 383.
(2) Burns, R. C.; Corbett, J. D. *Inorg. Chem.* **1981**, *20*, 4433.
(3) (a) Rudolph, R.; Wilson, W. L.; Taylor, R. C. *J. Am. Chem. Soc.* **1981**, *103*, 2480. (b) Eisenmann, B.; Schäfer, H.; Schrod, H. *Z. Naturforsch., B: Anorg. Chem., Org. Chem.* **1983**, *38B*, 921.
(4) Belin, C. H. E.; Charbonnel, M. M. *Inorg. Chem.* **1982**, *21*, 2504.
(5) (a) Krebs, B. *Angew. Chem., Int. Ed. Engl.* **1983**, *22*, 113. (b) Schäfer, H.; Eisenmann, B. *Rev. Inorg. Chem.* **1981**, *3*, 29.
(6) Burns, R. C.; Devereux, L. A.; Granger, P.; Schrobilgen, G. J. *Inorg. Chem.* **1985**, *24*, 2615.

0020-1669/87/1326-0741$01.50/0

Table I. ^{207}Pb, ^{125}Te, and ^{77}Se NMR Parameters and Satellite Intensities for the $Pb_2Ch_3^{2-}$ Anions

anion	chem shift, δ[a,b]			coupling constant $^1J_{^{207}Pb-Ch}$, Hz[a]		100(total satellite intens/central peak intens)[c]		
	^{207}Pb	^{77}Se	^{125}Te	$^{207}Pb-^{77}Se$	$^{207}Pb-^{125}Te$	^{207}Pb	^{77}Se	^{125}Te
$Pb_2Se_3^{2-}$	3290	−99.4		149		12 ± 1[d]	28[e]	
	(3353)	(−99.6)		(149)		(12)	(28)	
$Pb_2Se_2Te^{2-}$	2894	−190.0	−699.2	188	915	3 ± 1[e,f]	29 ± 1[e]	29 ± 3[d]
	(2832)	(−189.7)	(−700.5)	(188)	(915)	(4)	(28)	(28)
$Pb_2SeTe_2^{2-}$	2375	−279.7	−817.0	227	994	8 ± 1[d,f]	32 ± 1[e]	26 ± 2[d]
	(2311)	(−279.8)	(−814.4)	(227)	(993)	(8)	(28)	(28)
$Pb_2Te_3^{2-}$	1727		−927.1		1070	12 ± 1.5[e]		30 ± 3[d]
	(1790)		(−928.4)		(1070)	(13)		(28)
a[g]	3352.7	−99.6	−586.5	149.0	838.0			
b[g]	−520.8	90.15	−114.0	39.0	77.5			
R^2[g]	0.988	1.000	1.000	1.000	1.000			

[a] Calculated values in parentheses; estimated errors in Pb–Se and Pb–Te are ±2 and ±12 Hz, respectively. [b] Chemical shifts have been referenced at 24 °C with respect to the neat liquids $Pb(CH_3)_4$ (^{207}Pb), $Se(CH_3)_2$ (^{77}Se), and $Te(CH_3)_2$ (^{125}Te). [c] Theoretical ratio in parentheses. [d] Ratio measured from the integrated peak areas. [e] Ratio measured from the peak heights. [f] Value given for the ^{125}Te satellites only; the ^{77}Se satellites overlap extensively with the central peak. [g] Linear least-squares regression analysis of $\delta = a + bn$ and $^1J_{Pb-Ch} = a + bn$, where n = number of Te atoms in the anion and R^2 = correlation coefficient.

A significant portion of our present research in this area is directed toward extending the known series of classical polyanions and establishing the relationship between their structures and those of their related non classically bonded cluster species. In view of our recent successes in establishing the mixed series of classically bonded tin(IV) species $SnCh_3^{2-}$ (trigonal planar), $SnCh_4^{4-}$ (tetrahedral),[6] and $Sn_2Se_6^{4-}$ (D_{2h})[7] in en solution using NMR spectroscopy, we report here on the extension of these studies to the lead chalcogenide anions. As all of the previously established tin chalcogenide anions contain tin in its +4 oxidation state, it might be anticipated that by virtue of lead's propensity for the +2 oxidation state it should exhibit a novel chalcogenide anion chemistry of its own.

Results and Discussion

NMR Spectroscopy of the $Pb_2Se_{3-n}Te_n^{2-}$ ($n \leq 3$) Anions. The experimental approach involved the syntheses of the quaternary alloys $KPb_{0.54}Te_{0.33}Se_{0.67}$ and $KPb_{0.56}Te_{0.67}Se_{0.33}$ by fusion of the elements. Subsequent extraction in en in the presence of a slight excess of 2,2,2-crypt in all cases resulted in residual solid after extraction, but these residues were not investigated in view of the lack of data concerning the appropriate quaternary systems except to note that they were, like the initial alloy compositions themselves, hydrolytically unstable.

Structural Characterization by NMR Spectroscopy. Identification of the Zintl anions present in the en extracts was accomplished by direct NMR observation of the spin-$^1/_2$ nuclides ^{207}Pb (22.6%), ^{125}Te (6.99%), and ^{77}Se (7.58%) at their natural-abundance levels.

The solutions, when isolated from the alloy residues, yielded a total of four ^{207}Pb, three ^{125}Te, and three ^{77}Se environments with accompanying satellite spectra (Figures 1 and 2). In addition, the ^{77}Se spectrum exhibited one intense resonance without satellites. As the chemical shift is identical with the one observed from the extraction of K_2Se in en in the presence of 2,2,2-crypt, the signal is assigned to Se^{2-}.[6] A comparison of the magnitudes of the satellite doublet spacings in each spectrum yielded the one-bond scalar couplings $^1J_{^{207}Pb-^{77}Se}$ and $^1J_{^{207}Pb-^{125}Te}$, and from the latter it was possible to identify the set of ^{207}Pb, ^{125}Te, and ^{77}Se chemical shifts corresponding to each new species. Comparison of the satellite peak/central peak areas (integrated or peak height) ratios in the ^{207}Pb spectra with the calculated ratios gave the total number of Se or Te atoms bonded to each Pb environment. Owing to the smaller magnetogyric ratio of ^{77}Se compared to that of ^{125}Te, the former satellite lines were always innermost and were well-separated from the ^{125}Te lines. The number of Se atoms, m, or Te atoms, n, bonded to each Pb atom was found to be n = 0–3 and m = 0–3 such that $n + m = 3$. Since only four lead-containing species were observed, the species formed are assigned to the four

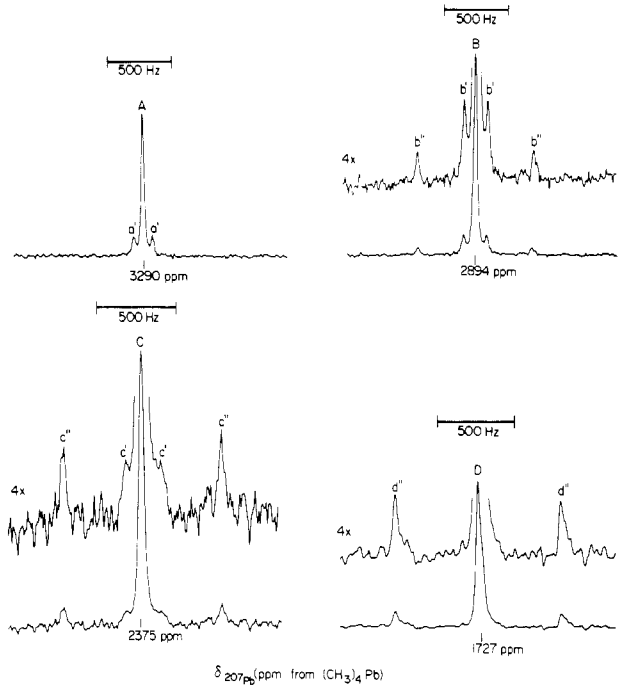

Figure 1. ^{207}Pb NMR spectra of the $Pb_2Ch_3^{2-}$ series of anions, obtained at 52.174 MHz in en solvent: (A) $Pb_2Se_3^{2-}$; (B) $Pb_2Se_2Te^{2-}$; (C) $Pb_2SeTe_2^{2-}$; (D) $Pb_2Te_3^{2-}$. Peaks labeled a′, b′, and c′ denote ^{77}Se satellites; peaks labeled b″, c″, and d″ denote ^{125}Te satellites.

mixed Se/Te species $Pb_xSe_{3-n}Te_n^{z-}$. Additional information concerning the nature of these species is obtained from the lead satellite peak/central peak area ratios in the ^{77}Se NMR spectra and the corresponding ratios in the ^{125}Te NMR spectra, allowing us to conclude that the three chalcogen atoms were equivalently bonded to two lead atoms (Table I). As the most common and stable oxidation state of lead is +2 by virtue of the inertness of the $6s^2$ pair, and each chalcogen atom may be assumed to possess a formal oxidation state of −2, we can infer that the anions are dinegative; that is, they are the series of dinuclear lead chalcogenide anions $Pb_2Se_{3-n}Te_n^{2-}$. In addition, it is found that plots of the ^{207}Pb, ^{77}Se, and ^{125}Te chemical shifts and $^{207}Pb-^{77}Se$ and $^{207}Pb-^{125}Te$ coupling constants vs. the number of chalcogen atom substituents are near linear, further indicating the series is homologous and isostructural (see below). The structure, which is consistent with the NMR findings, is based upon a trigonal bipyramid with the chalcogen atoms occupying the equatorial positions and bonded to two Pb atoms in the apical positions (structure I).

Chemical Shift Trends. The general trend found in this work with respect to the electropositive Pb atom nucleus is that a

(7) Burns, R. C.; Devereux, L. A.; Schrobilgen, G. J., unpublished results.

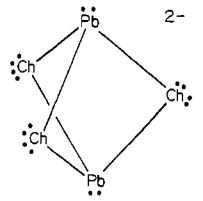

I

decrease in the total electron-withdrawing ability of the ligand atoms attached to the lead atoms results in a near-additive increase in the lead shielding (Table I). This behavior parallels that exhibited by the central atom nuclei in other classically bonded chalcogenide anions, i.e., $CdCh_2^{2-}$, $HgCh_2^{2-}$, $Tl_2Ch_2^{2-}$, $TlCh_3^{3-}$, $SnCh_3^{2-}$, and $SnCh_4^{4-}$.[6] For the $Pb_2Se_{3-n}Te_n^{2-}$ series of anions, the ^{125}Te and ^{77}Se chemical shift trends, like that of ^{207}Pb, also show a near-additive decrease in their shieldings on increasing the total ligand electronegativity (Table I). Interestingly, these trends in chalcogen shieldings are opposite to those previously observed in the Cd, Hg, Tl, and Sn series[6] of chalcogenide anions. The chemical shift trend in all three nuclides are those expected on the basis of simple inductive effects caused by varying the number and kind of chalcogen atoms in a particular geometry and can be correlated with a change of electron density on the nucleus in question to give a diamagnetic contribution to the shielding. However, the observed changes appear to be too large to be attributed to this inductuve effect so that the paramagnetic term in Ramsey's shielding expression (eq 1)[8] must be primarily

$$\sigma = \sigma^d + \sigma^p \quad (1)$$

responsible for the observed chemical shift trends. In this equation, σ^d involves free rotation of electrons about the nucleus and σ^p describes the restriction to their rotation caused by other electrons and other nuclei in the molecule.

For the series of $Pb_2Se_{3-n}Te_n^{2-}$ anions, each component nucleus was subjected to a linear least-squares regression analysis of its chemical shift as a function of n, the number of tellurium substituent atoms when $n \leq 3$. It was found that the calculated values for the chemical shifts were generally in excellent agreement with the observed shifts (Table I). Thus, their additivity supports the assignments of these species using the criteria originally used for their identification. The additivity of chemical shifts in this series of anions is also illustrated by the correlation factors (also given in Table I). This agreement is helped by the fact that little or no concentration dependence of chemical shifts (or coupling constants) was noted for any of these species. Moreover, additivity among chemical shifts for homologous series of classically bonded chalcogenide Zintl anions appears to be a consistent feature.[6]

Coupling Constants (^1J, ^1K, and Relativistically Corrected ^1K). The spin–spin coupling constants $^1J_{^{207}Pb-^{125}Te}$ and $^1J_{^{207}Pb-^{77}Se}$ are also directly additive and increase with decreasing total electron-withdrawing ability of the ligand atoms or n, the number of tellurium atoms. The trend is the same as that observed previously for $HgCh_2^{2-}$ but opposite to those trends observed for $TlCh_3^{3-}$, $SnCh_3^{2-}$, and $SnCh_4^{4-}$.

The nuclear spin–spin coupling interaction results from a correlation of nuclear spins arising out of their interaction with the surrounding electrons. In high-resolution NMR spectroscopy spin–spin coupling is usually dominated by the Fermi contact mechanism and can be discussed in terms of the formalism developed by Pople and Santry[9] (eq 2, where all symbols have their

$$^1J_{AB} = \frac{16\pi^2}{9h}\left(\frac{g\beta h}{2\pi}\right)^2 \gamma_A\gamma_B|\psi_{ns,A}(0)|^2|\psi_{ns,B}(0)|^2\pi_{AB} \quad (2)$$

usual meanings). From the latter formalism, the observed (one-bond) coupling constant $^1J_{AB}$ is dependent upon the nuclear properties of the coupled nuclei, i.e., the magnetogyric ratios γ_A and γ_B, and on electronic terms, i.e. $|\psi_{ns,A}(0)|^2$ and $|\psi_{ns,B}(0)|^2$, the

(8) Ramsey, N. F. *Phys. Rev.* **1950**, *78*, 699.
(9) Pople, J. A.; Santry, D. P. *Mol. Phys.* **1964**, *8*, 1.

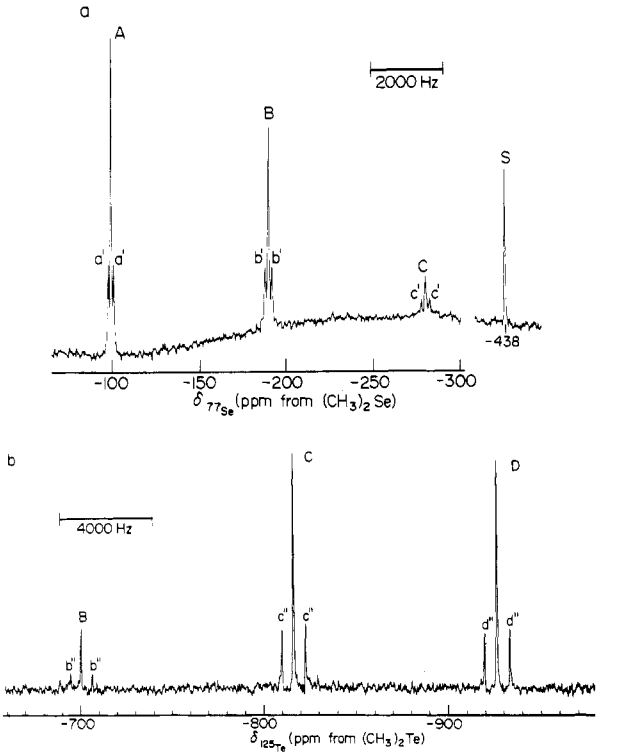

Figure 2. (a) ^{77}Se NMR spectrum obtained at 47.704 MHz in en solvent and (b) ^{125}Te NMR spectrum obtained at 78.917 MHz in en solvent of the $Pb_2Ch_3^{2-}$ series of anions: (A) $Pb_2Se_3^{2-}$; (B) $Pb_2Se_2Te^{2-}$; (C) $Pb_2SeTe_2^{2-}$; (D) $Pb_2Te_3^{2-}$. Peaks labeled a′, b′, c′, b″, c″ and d″ denote ^{207}Pb satellites and correspond to the labeling scheme used in Figure 1. Peak S corresponds to Se^{2-}.

Table II. Reduced Coupling Constants, ^1K, and Relativistically Corrected Reduced Coupling Constants, $^1K_{RC}$, for the Anions $Pb_2Ch_3^{2-}$ and $Tl_2Ch_2^{2-}$

	$^1K^a$		$^1K_{RC}{}^{a,b}$	
anion	M–Se	M–Te	M–Se	M–Te
$Pb_2Se_3^{2-}$	31.1		8.74	
$Pb_2Se_2Te^{2-}$	39.2	115	11.0	26.0
$Pb_2SeTe_2^{2-}$	47.4	125	13.3	28.3
$Pb_2Te_3^{2-}$		135		30.4
$Tl_2Se_2^{2-}$	171		48.4	
Tl_2SeTe^{2-}	159	165	45.0	37.5
$Tl_2Te_2^{2-}$		366		83.0

[a] K and K_{RC} are in SI units of N A^{-2} m^{-3} when J is measured in Hz. All ^1K and $^1K_{RC}$ values are to be multiplied by a factor of 10^{20}. M = Pb or Tl. [b] Linear least-squares regression analyses of $(^1K_{Pb-Ch})_{RC} = a_{Ch} + b_{Ch}n$, where n = number of Te atoms in the anion and R^2 = correlation coefficient: $a_{Se} = 8.73$, $b_{Se} = 2.28$, $R^2 = 1.000$; $a_{Te} = 23.80$, $b_{Te} = 2.20$, $R^2 = 1.000$. All a_{Ch} and b_{Ch} values are to be multiplied by a factor of 10^{20}.

s-electron densities for the valence ns orbitals at their respective nuclei A and B, and π_{AB}, the mutual polarizability of s orbitals on A and B. In order to look at structurally related effects on the spin–spin coupling, it is necessary to remove the nuclear dependence. This is accomplished by defining the reduced coupling constant $^1K_{AB}$ (eq 3), which gives a better representation of

$$^1K_{AB} = \frac{4\pi^2}{h\gamma_A\gamma_B}{}^1J_{AB} \quad (3)$$

electronic environments in the series of anions under discussion (Table II). Factoring out the nuclear-dependent terms of the directly bonded coupled nuclei in eq 3 gives comparable reduced coupling constants within each chalcogen series, $^1K_{Pb-Se}$ and $^1K_{Pb-Te}$. There is, however, a considerable difference between individual $^1K_{Pb-Se}$ and $^1K_{Pb-Te}$ values, and such differences would, as a consequence of eq 3, be expected to be dominated by the s-electron density term. As we have already noted in a previous

discussion of reduced spin–spin couplings for classically bonded Zintl anions, this approach does not take relativistic effects on s-electron density into account. These effects can be extremely important when making comparisons between Fermi contact dominated spin–spin couplings involving heavy elements such as Pb, Te, and Se. In the case of Pb in particular, the relativistic effect on s-electron density is very large as this nucleus with $Z = 82$ is near Au ($Z = 79$), which exhibits the maximum for relativistic effects.

We have previously noted and illustrated a method for factoring out relativistic effects on $|\psi_{ns}(0)|^2$ and associated Fermi contact dominated heavy-element spin–spin couplings in $CdCh_2^{2-}$, $HgCh_2^{2-}$, $TlCh_3^{3-}$, $SnCh_3^{2-}$, and $SnCh_4^{4-}$.[6] The correction for a given element is accomplished by considering the ratio $(|\psi_{ns}(0)|^2)_{rel}/(|\psi_{ns}(0)|^2)_{nonrel}$ for a particular element. Values for relativistic and nonrelativistic s-electron densities taken from the work of Pyykkö and Wiesenfeld give the following ratios:[10] Pb, 3.080; Te, 1.439; Se, 1.155. Thus, for the $Pb_2Se_{3-n}Te_n^{2-}$ anions studied, in the most extreme case of $^1K_{Pb-Te}$, a factor of 4.431 for a relativistic correction would apply, while in the case of $^1K_{Pb-Se}$, a factor of 3.557 would apply. The relativistically corrected reduced coupling constants $(^1K_{Pb-Se})_{RC}$ and $(^1K_{Pb-Te})_{RC}$ are given in Table II. Unlike the relativistically corrected reduced coupling constants in the previous study, there is a large disparity between $(^1K_{Pb-Se})_{RC}$ and $(^1K_{Pb-Te})_{RC}$ values with a maximum variation occurring for the couplings in the $Pb_2Se_3^{2-}$ and $Pb_2Te_3^{2-}$ anions (248%) and a minimum variation corresponding to the $Pb_2Se_2Te^{2-}$ and $Pb_2SeTe_2^{2-}$ anions (96%). In general, $(^1K_{Pb-Se})_{RC}$ and $(^1K_{Pb-Te})_{RC}$ are, respectively, approximately $^1/_{20}$ to $^1/_3$ the magnitudes of the $^1K_{RC}$ values for $SnCh_4^{4-}$, $SnCh_3^{2-}$, and $TlCh_3^{3-}$, and within the latter series variations in $^1K_{RC}$ are seldom more than 30%.

A previous study of $(CH_3)_3PbSeCH_3$ has yielded a $^1J_{^{207}Pb-^{77}Se}$ value of -1170 ± 100 Hz.[11] The calculated absolute value of $(^1K_{Pb-Se})_{RC} = 68.6 \times 10^{20}$ N A^{-2} m^{-3} is consistent with the high s character anticipated for this sp^3-hybridized lead(IV) species and, in fact, agrees reasonably well with $(^1K_{Sn-Te})_{RC} = (89.9–104.1) \times 10^{20}$ N A^{-2} m^{-3} and $(^1K_{Sn-Te})_{RC} = (98.2–123.0) \times 10^{20}$ N A^{-2} m^{-3} for the sp^3-hybridized series. This value contrasts with the p-bonded lead(II) cage series $Pb_2Ch_3^{2-}$ where $(^1K_{Pb-Se})_{RC}$ and $(^1K_{Pb-Te})_{RC}$ are much smaller and are in the ranges $(8.74–13.3) \times 10^{20}$ and $(26.0–30.4) \times 10^{20}$ N A^{-2} m^{-3}, respectively. It is therefore apparent that the s characters of the metal–chalcogen bonds are greatly diminished in the trigonal-bipyramidal lead(II) anion series $Pb_2Ch_3^{2-}$ when compared to those of other classically bonded Zintl species and lead(IV) species. The apparent diminution of s character in the Pb–Ch bonds of $Pb_2Ch_3^{2-}$ may arise from the inherent clusterlike character of the anions, which may rely more heavily upon the use of pure p orbitals for the skeletal bonding. Alternatively, the effect may be viewed as a consequence of geometrical constraint in a classically bonded system. It appears that the Pb–Ch–Pb and Ch–Pb–Ch angles may be too small to accommodate optimal s-orbital participation in the classical bonding scheme, causing the need to invoke greater p-orbital character in the bonding (see Crystal Structure). Furthermore, due to the inert nature of the 6s^2 core of lead(II), the s character of the bonds is expected to be greatly diminished. Thus, the $^1K_{RC}$ values are overall significantly smaller than in the previously cited mononuclear cases where the formal oxidation states of the electropositive central metals are high, geometrical constraints are lacking, and the valence s-electron pairs of the central metal atoms are formally involved in classical hybridization schemes possessing significant s character, i.e., sp (MCh_2^{2-}), sp^2 (MCh_3^{z-}, $z = 2, 3$), and sp^3 (MCh_4^{4-}).

Moreover, when the number of Te atom substituents (n) is made the independent variable and is in that against $(^1K_{Pb-Ch})_{RC}$, two parallel linear relationships result (Table II), whose positive slopes are 2.28×10^{20} (Se series) and 2.20×10^{20} N A^{-2} m^{-3} (Te series) per Te atom substituent. Interestingly, the effect for each substituent atom change on the s-orbital contribution in both series of couplings is essentially the same. Thus, the difference $(^1K_{Pb-Te})_{RC} - (^1K_{Pb-Se})_{RC} \approx 15 \times 10^{20}$ N A^{-2} m^{-3} is essentially constant by virtue of the lines' parallelism and appears to be an indication of greater s-orbital involvement in the Pb–Te bond in comparison to that in the Pb–Se bond. The difference, however, is small when compared with typical ^1K values, which range between $\sim 10^{22}$ and 10^{23} N A^{-2} m^{-3}. From electronegativity differences in the $Pb_2Ch_3^{2-}$ anion series we would expect the angle trends Se–Pb–Se < Te–Pb–Te and Pb–Se–Pb > Pb–Te–Pb. Each substitution of a less electronegative Te atom for a Se atom then leads to an enhancement of s character in the Pb and Ch sets of hybridized valence orbitals used in bonding by increasing the average Ch–Pb–Ch angles and hence the average Pb–Ch bond s character by a similar amount. Alternatively, if the Pb 6s^2 electrons are regarded as virtually inert, then the above trends in $(^1K_{Pb-Ch})_{RC}$ as the larger Te substituent atoms are progressively added may be mostly attributed to changes in s-character of the hybridized valence orbitals of the chalcogen and could be regarded as largely due to a chalcogen size effect.

The butterfly-shaped $Tl_2Te_2^{2-}$ anion[12] may be regarded as a close structural relative to the $Pb_2Ch_3^{2-}$ series, in that one of the vertices occupied by a chalcogen atom has been left vacant. In $Tl_2Te_2^{2-}$ the Te–Tl–Te bond angles (average 96.64 (8)°; cf. Tl–Te–Tl = 75.07 (7)°) are, as in $Pb_2Se_3^{2-}$, considerably less than the ideal tetrahedral angle and are, in fact, closer to the ideal 90° angle indicative of metal pure p-valence-orbital involvement in the bonding scheme and inertness of the 6s^2 pair. Again, this view is supported by comparisons of $(^1K_{Tl-Ch})_{RC}$ among the trigonal-planar (formally sp^2-hybridized Tl valence orbitals) $TlCh_3^{2-}$ and the $Tl_2Ch_2^{2-}$ series (Table II), which have been extensively studied in solution by multinuclear magnetic resonance spectroscopy.[6] The classical sp^2-hybridized $TlCh_3^{3-}$ species are found to possess substantially larger $(^1K_{Tl-Ch})_{RC}$ values than the $Tl_2Ch_2^{2-}$ species. The validity of assigning an sp^2 hybridization scheme to $TlCh_3^{3-}$ presumes extensive involvement of the 6s^2 core in bonding and is supported by the close similarity of $(^1K_{Sn-Ch})_{RC}$ values of the $SnCh_3^{2-}$ series ($(1.36–1.74) \times 10^{22}$ N A^{-2} m^{-3}) and those of the $TlCh_3^{3-}$ series ($(1.46–1.84) \times 10^{22}$ N A^{-2} m^{-3}). As a consequence, two further interesting comparisons between the $Tl_2Ch_2^{2-}$ and $Pb_2Ch_3^{2-}$ series can be made: (1) the increases in $(^1K_{M-Te})_{RC}$ with increasing Te number are presumed to arise from greater 6s metal orbital and/or greater chalcogen s-orbital involvement due to enlargement of the Ch–M–Ch angles upon Te substitution in both series; (2) overall, the values of $(^1K_{Tl-Ch})_{RC}$ are significantly larger than $(^1K_{Pb-Ch})_{RC}$ values, which correlates well with Ch–M–Ch bond angles in $Pb_2Se_3^{2-}$ (⟨Se–Pb–Se⟩ = 89.8°) and $Tl_2Te_2^{2-}$ (⟨Te–Tl–Te⟩ = 96.6°)[12] and which argues for significantly higher p character for the M–Ch bonds in the $Pb_2Ch_3^{2-}$ series.

Crystal Structure. Crystals of (2,2,2-crypt-K$^+$)$_2$Pb$_2$Se$_3^{2-}$ consist of an ordered assembly of discrete cryptated potassium ions and $Pb_2Se_3^{2-}$ anions. The final positional and thermal parameters for the non-hydrogen atoms in (2,2,2-crypt-K$^+$)$_2$Pb$_2$Se$_3^{2-}$ are listed in Table III. Selected bond distances and angles for the $Pb_2Se_3^{2-}$ anions and the 2,2,2-crypt-K$^+$ cations are given in Table IV. The geometries of the cryptated potassium ions are normal with K···O and K···N distances (2.75 (3)–3.08 (3) Å) comparable to those observed in (2,2,2-crypt-K$^+$)$_2$Tl$_2$Te$_2^{2-}$·en (2.69 (2)–3.02 (2) Å)[12] and (2,2,2-crypt-K$^+$)$_2$Te$_3^{2-}$·en (2.76 (3)–3.02 (4) Å).[13] A stereoview of the crystal packing is given in Figure 3 (supplementary material) and indicates that each anion is completely surrounded by 10 (2,2,2-crypt-K$^+$) cations.

The most interesting aspect of the structure is the anion: a flattened trigonal-bipyramidal shape of approximately D_{3h} symmetry (Figure 4). The Pb atoms are in apical positions and the Se atoms in equatorial positions in agreement with the gross structure deduced from the solution NMR studies. Perhaps one of the more interesting features of the $Pb_2Se_3^{2-}$ structure is the

(10) Pyykkö, P.; Wiesenfeld, L. *Mol. Phys.* **1981**, *43*, 557.
(11) Kennedy, J. D.; McFarlane, W.; Wrackmeyer, B. *Inorg. Chem.* **1976**, *15*, 1299.
(12) Burns, R. C.; Corbett, J. D. *J. Am. Chem. Soc.* **1981**, *103*, 2627.
(13) Cisar, A.; Corbett, J. D. *Inorg. Chem.* **1977**, *16*, 632.

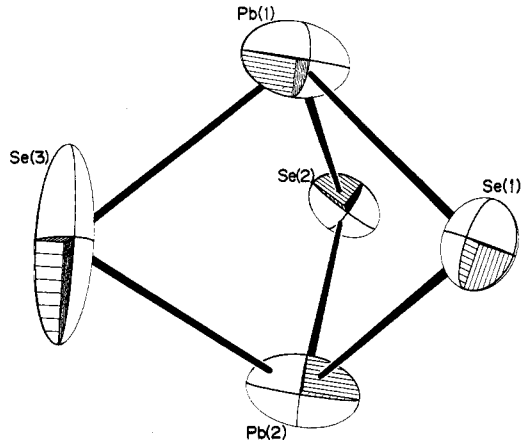

Figure 4. ORTEP view of the $Pb_2Se_3^{2-}$ anion including the atom-numbering scheme with ellipsoids drawn at 50% probability.

short Pb(1)–Pb(2) distance of 3.184 (3) Å. While the equatorial Se···Se distances of 3.81, 3.89, and 3.95 Å are close to van der Waals contact distances (3.8 Å) and comply with localized valence bond structure I, the Pb(1)–Pb(2) distance is significantly less than the van der Waals contact (4.0 Å) and intermediate with respect to the bonding Pb–Pb distances in the structurally related homopolyatomic anion Pb_5^{2-} (equatorial–equatorial distances, 3.24–3.32 Å; equatorial–axial distances, 3.00–3.08 Å; axial–axial distance, 4.70 Å).[14] Moreover, the Pb–Pb distance in Ph_6Pb_2 is 2.83 (1) Å[15] whereas the shortest Pb–Pb distances in the cluster cation in α-$(Pb_6O(OH)_6^{4+})(ClO_4^-)_4 \cdot H_2O$[16] are ≥3.440 (5) Å and the nearest-neighbor distance in metallic lead is ca. 3.49 Å.[24] While it is tempting to consider the present Pb(1)–Pb(2) distance to be a bonding interaction, the short Pb–Pb distance may result from geometrical constraints arising within the trigonal-pyramidal $PbSe_3$ moiety (see below). The Pb–Se bond lengths in $Pb_2Se_3^{2-}$ (which vary widely from 2.726 (5) to 2.792 (8) Å (average 2.751 Å) due to the anisotropy in the thermal parameters of the Pb and Se atoms) are similar to the Pb–Se distances in the $Pb(SePh)_3^-$ anion (2.727, 2.733, and 2.762 (1) Å)[17] while significantly longer than the sum of the covalent radii (2.67 Å). The last value is derived from the covalent radius of Se (1.17 Å) and the tetrahedral radius of Pb (1.44 Å).[18] Other reported Pb^{II}–Se distances for coordination numbers of 6 and higher at the lead atom are in the range 2.80–3.30 Å.[19] However, when the metallic radius of Pb(II) (1.54 Å)[20] is employed, substantially better agreement is obtained (2.71 Å) with our findings and those of Dean et al.[17] for the $Pb(SePh)_3^-$ anion, although we note that the considerably contracted Pb–Se–Pb angles (70.4 (1), 70.8 (1), and 70.9 (1)°) would imply that the Pb–Se bonds in the present anion are "bent". This would then make the Se–Pb–Se angles of $Pb_2Se_3^{2-}$ (87.1 (2)–91.6 (1)°) even more comparable to those in the less constrained $Pb(SePh)_3^-$ anion (88.8–96.6°).[17]

Bonding in $Pb_2Ch_3^{2-}$ (Ch = Se and/or Te). The proposal, discussed in the section dealing with the NMR spectroscopy of $Pb_2Ch_3^{2-}$ anions, that reduced s-character in the Pb–Ch bonding scheme is responsible for the low values of the relativistically corrected reduced spin–spin coupling constants $(^1K_{Pb-Ch})_{RC}$ in these anions is further supported by the X-ray crystal structure of $Pb_2Se_3^{2-}$. In this vein, we note that the Se–Pb–Se angles are close to 90°, in accord with substantial 6p-orbital involvement on lead. Similarly, the Pb–Se–Pb bond angles (70.4 (1), 70.8 (1), and 70.9 (1)°) are considerably compressed from the ideal angle of 90° and may be described as bent although the Se–Pb–Se angles are more normal. In the butterfly-shaped anion $Tl_2Te_2^{2-}$,[12] the Tl–Te–Tl angles are again much smaller than 90° (74.76 (7) and 75.38 (7)°) as a consequence of minimization of nonbonded interactions and the predominance of p-orbital bonding for thallium rather than tellurium. Similar arguments regarding relative s- and p-orbital energies may be made for Pb–Se and Pb–Te bonding.

Table III. Final Atomic Positional (×10⁴) and Thermal (×10³) Parameters with Estimated Standard Deviations in Parentheses

atom	x	y	z	U or U_{eq}, Å²
Pb(1)	3314 (2)	1150.1 (5)	1299 (2)	82 (2)[a]
Pb(2)	241 (2)	1210.3 (5)	1343 (2)	67 (1)[a]
Se(1)	1832 (4)	1402.0 (9)	−408 (4)	48 (3)[a]
Se(2)	1872 (4)	1403.9 (10)	3048 (4)	53 (3)[a]
Se(3)	1530 (10)	703.8 (11)	1267 (6)	150 (8)[a]
K(1)	1768 (8)	4434 (2)	1276 (7)	43 (5)[a]
K(2)	1839 (8)	2923 (2)	1350 (7)	41 (5)[a]
N(11)	3411 (35)	4416 (8)	−872 (32)	66 (11)
C(12)	2604 (42)	4348 (9)	−1931 (38)	62 (13)
C(13)	1646 (41)	4108 (9)	−1742 (39)	61 (13)
O(14)	875 (28)	4145 (6)	−762 (26)	68 (9)
C(15)	21 (35)	3915 (8)	−491 (33)	42 (10)
C(16)	−1016 (36)	4005 (8)	275 (32)	47 (11)
O(17)	−503 (23)	4097 (5)	1429 (21)	42 (7)
C(18)	−1561 (40)	4148 (9)	2177 (35)	59 (12)
C(19)	−877 (33)	4210 (7)	3352 (29)	34 (9)
N(110)	81 (31)	4457 (7)	3421 (29)	53 (9)
C(111)	928 (45)	4425 (10)	4470 (41)	72 (14)
C(112)	1851 (39)	4164 (9)	4248 (36)	55 (12)
O(113)	2747 (25)	4230 (6)	3393 (23)	51 (7)
C(114)	3817 (44)	4048 (10)	3235 (42)	71 (14)
C(115)	4716 (36)	4134 (9)	2465 (33)	46 (11)
O(116)	4103 (27)	4143 (6)	1320 (25)	63 (8)
C(117)	5082 (35)	4226 (8)	454 (31)	42 (10)
C(118)	4463 (40)	4256 (9)	−813 (36)	56 (12)
C(119)	3897 (46)	4675 (10)	−1087 (43)	73 (14)
C(120)	3037 (49)	4950 (11)	−962 (44)	84 (16)
O(121)	2688 (36)	4952 (8)	237 (33)	94 (11)
C(122)	1752 (69)	5157 (15)	256 (60)	137 (26)
C(123)	1449 (70)	5182 (16)	1406 (61)	154 (30)
O(124)	643 (29)	4963 (6)	1996 (27)	70 (9)
C(125)	199 (49)	4945 (11)	3226 (45)	82 (16)
C(126)	−586 (39)	4728 (8)	3499 (36)	51 (11)
N(21)	1973 (31)	2924 (7)	4030 (28)	51 (9)
C(22)	688 (49)	3020 (11)	4482 (47)	92 (17)
C(23)	241 (45)	3284 (10)	3804 (38)	71 (14)
O(24)	−201 (26)	3149 (6)	2695 (24)	56 (8)
C(25)	−1002 (40)	3339 (9)	2007 (35)	59 (12)
C(26)	−1376 (40)	3190 (9)	833 (36)	60 (12)
O(27)	−237 (22)	3171 (5)	218 (20)	38 (6)
C(28)	−580 (39)	3030 (9)	−900 (34)	54 (12)
C(29)	658 (42)	3079 (10)	−1691 (40)	67 (13)
N(210)	1755 (30)	2894 (6)	−1336 (26)	46 (9)
C(211)	1500 (45)	2588 (9)	−1715 (41)	67 (13)
C(212)	2151 (42)	2408 (9)	−967 (36)	61 (13)
O(213)	1683 (29)	2392 (6)	152 (27)	72 (9)
C(214)	2170 (51)	2160 (11)	940 (42)	85 (16)
C(215)	1541 (51)	2195 (11)	2025 (45)	89 (17)
O(216)	2019 (25)	2406 (6)	2723 (24)	55 (8)
C(217)	1491 (46)	2421 (10)	3761 (39)	73 (15)
C(218)	2114 (41)	2653 (8)	4454 (36)	55 (12)
C(219)	3015 (44)	3132 (10)	4400 (43)	75 (15)
C(220)	4180 (42)	3093 (9)	3586 (37)	63 (13)
O(221)	3857 (28)	3195 (6)	2472 (26)	67 (9)
C(222)	4967 (48)	3261 (11)	1749 (44)	86 (16)
C(223)	4522 (45)	3373 (10)	672 (39)	73 (14)
O(224)	3884 (26)	3161 (6)	69 (24)	60 (8)
C(225)	3501 (45)	3259 (10)	−1083 (38)	73 (15)
C(226)	2971 (48)	3016 (11)	−1852 (47)	90 (17)

[a] Atom refined anisotropically and given in terms of its equivalent isotropic thermal parameter.

(14) Edwards, P.; Corbett, J. D. *Inorg. Chem.* **1977**, *16*, 903.
(15) Preut, H.; Haupt, H. J.; Huber, F. *Z. Anorg. Allg. Chem.* **1972**, *388*, 165.
(16) Olin, A.; Söderquist, R. *Acta Chem. Scand.* **1972**, *26*, 3505.
(17) Dean, P. A. W.; Vittal, J. J.; Payne, N. C. *Inorg. Chem.* **1984**, *23*, 4232.
(18) Cotton, F. A.; Wilkinson, G. *Advanced Inorganic Chemistry*, 4th ed.; Wiley: New York, 1980; p 375.
(19) (a) Iglesis, J. E.; Steinfink, H. *J. Solid State Chem.* **1973**, *6*, 93. (b) Krebs, B. *Z. Anorg. Allg. Chem.* **1973**, *396*, 137. (c) Potel, M.; Robert, B.; Padiou, J. *Mater. Res. Bull.* **1975**, *20*, 205. (d) Guillevic, P. J.; Lesbrat, H.; Grandjean, D. *Acta Crystallogr., Sect. B: Struct. Crystallogr. Cryst. Chem.* **1976**, *B32*, 1342. (e) Klee, W.; Shafter, H. *Mater. Res. Bull.* **1980**, *15*, 1033.
(20) Pauling, L. *The Nature of the Chemical Bond*, 3rd ed.; Cornell University Press: Ithaca, NY, 1960; Chapter 11, p 420.

Table IV. Selected Bond Lengths (Å) and Bond Angles (deg)

(i) $Pb_2Se_3^{2-}$ Anion

Bond Lengths

Pb(1)···Pb(2)	3.184 (3)	Pb(1)–Se(2)	2.768 (5)	Pb(2)–Se(1)	2.746 (5)
Pb(1)–Se(1)	2.743 (5)	–Se(3)	2.792 (8)	–Se(2)	2.726 (5)
				–Se(3)	2.729 (7)

Bond Angles

Se(1)–Pb(1)–Se(2)	91.6 (1)	Se(1)–Pb(2)–Se(2)	92.4 (1)	Pb(1)–Se(1)–Pb(2)	70.9 (1)
–Se(3)	87.1 (2)	–Se(3)	88.3 (2)	Pb(1)–Se(2)–Pb(2)	70.8 (1)
Se(2)–Pb(1)–Se(3)	88.7 (2)	Se(2)–Pb(2)–Se(3)	90.8 (2)	Pb(1)–Se(3)–Pb(2)	70.4 (1)

(ii) K^+ Ions

	$n = 1$	$n = 2$		$n = 1$	$n = 2$
Bond Lengths					
K(n)–N(n1)	2.99 (4)	3.07 (3)	K(n)–O(n13)	2.79 (3)	2.86 (3)
–O(n4)	2.85 (3)	2.82 (3)	–O(n16)	2.77 (3)	2.90 (3)
–O(n7)	2.84 (3)	2.76 (2)	–O(n21)	2.87 (4)	2.75 (3)
–N(n10)	3.02 (3)	3.08 (3)	–O(n24)	2.86 (3)	2.81 (3)
Bond Angles					
N(n1)–K(n)–O(n4)	59.8 (9)	59.1 (8)	O(n7)–K(n)–O(n13)	92.9 (8)	95.9 (8)
–O(n7)	120.4 (9)	120.0 (8)	–O(n16)	116.2 (8)	131.0 (8)
–N(n10)	179.2 (10)	177.3 (9)	–O(n21)	140.7 (9)	127.4 (8)
–O(n13)	119.9 (9)	118.8 (9)	–O(n24)	97.5 (8)	99.9 (8)
–O(n16)	60.3 (9)	57.1 (8)	N(n10)–K(n)–O(n13)	61.0 (8)	58.7 (8)
–O(n21)	59.7 (10)	60.3 (9)	–O(n16)	120.5 (9)	120.3 (8)
–O(n24)	119.5 (10)	119.4 (9)	–O(n21)	120.0 (10)	120.2 (9)
O(n4)–K(n)–O(n7)	61.2 (8)	61.0 (7)	–O(n24)	60.0 (9)	60.9 (8)
–N(n10)	119.7 (9)	122.9 (8)	O(n13)–K(n)–O(n16)	60.2 (8)	61.9 (8)
–O(n13)	131.3 (9)	123.4 (9)	–O(n21)	122.1 (10)	132.1 (9)
–O(n16)	93.2 (9)	93.8 (8)	–O(n24)	101.3 (9)	98.0 (9)
–O(n21)	100.0 (10)	97.9 (9)	O(n16)–K(n)–O(n21)	97.9 (10)	95.2 (8)
–O(n24)	121.3 (9)	134.4 (8)	–O(n24)	140.9 (9)	124.7 (8)
O(n7)–K(n)–N(n10)	59.3 (8)	62.1 (8)	O(n21)–K(n)–O(n24)	61.2 (10)	59.3 (9)

The simplest way of looking at the bonding in the $Pb_2Se_3^{2-}$ anion is to note the similarity between the Pb–Se distances and Se–Pb–Se angles in this anion and those in the $Pb(SePh)_3^-$ anion,[17] in which the lead atom possesses the classical trigonal-pyramidal coordination attributable to an AX_3E arrangement of three bond pairs and a lone pair about Pb, and to consider the inherent trigonal-pyramidal geometry of each of the $PbSe_3$ moieties of the trigonal-bipyramidal $Pb_2Se_3^{2-}$ anion as giving rise to the short apex–apex Pb–Pb distance. Moreover, the close similarity of the ^{207}Pb chemical shift of $Pb_2Se_3^{2-}$ (3290 ppm) compared to those of the structurally related Pb(II) ions $Pb(SePh)_3^-$ (3188 ppm)[17,21] and $Pb[SeP(C_6H_{11})_3]_3^{2+}$ (3011 ppm)[22] is also noteworthy and supports the view that the bonding to Pb in all three species is very similar. Unfortunately, the ^{207}Pb–^{77}Se coupling constant has not been observed in either of the last two ions. On the basis of these considerations, structure I can be drawn to represent the bonding.

Alternatively, we can use cluster/multicenter bonding arguments and isolobal relationships in drawing an analogy between the $Pb_2Se_3^{2-}$ anion structure and a recently published structure of $Bi_2[W(CO)_5]_3$.[23] In the first case, after one electron pair is allowed for each Pb and Se atom, there remain 18 electrons for cluster bonding. This number of electrons is consistent with a hypo cluster based on an eight-vertex polyhedron with three vertices missing:[24] in the present case, a hexagonal bipyramid with three equatorial positions missing. In the second case, we note the isolobal relationship between Se and $W(CO)_5$ and that Bi_2 and Pb_2^{2-} are isoelectronic. In the structure of $Bi_2[W(CO)_5]_3$ there is a Bi_2W_3 moiety of D_{3h} symmetry in which the Bi–Bi distance of 2.815 (7) Å is 0.26 Å shorter than that in Bi metal (3.071 Å) and the Bi–Wi–Bi angle is 54°. In $Pb_2Se_3^{2-}$ the Pb–Pb distance is 0.31 Å less than the nearest-neighbor distance in Pb metal (3.49 Å).[24]

The two bonding schemes for the $Pb_2Se_3^{2-}$ anion described above can be reconciled by considering only the 4p and 6p valence orbital energies of Se and Pb (−10.8 and −6.5 eV, respectively[26]) in a simplified molecular orbital description. As already shown by the NMR spin–spin coupling results, the lead $6s^2$ core is considered to be inert. The dissociation energy of the diatomic molecule Pb_2 has been measured in the gas phase and found to be 1.0 eV.[27] The dissociation energy of the hypothetical Pb_2^{2-} ion can therefore be estimated to have a maximum of 1.5 eV if we consider the energy of each Pb–Pb bond pair to be 0.5 eV. As a consequence, the 4p atomic orbitals of Se are lower in energy than the bonding molecular orbital of Pb_2^{2-} by at least 3.0 eV. At a large separation of the Se atoms, the species would be better represented as $[Pb^{2+}]_2[Se^{2-}]_3$ rather than as $[Pb_2^{2-}][Se]_3$. Therefore, in the cluster multicenter bonding description, where two Pb/Se valence p orbitals are tangential and one is radial, the six filled bonding molecular orbitals (a_1', a_2'', e', and e'') would result in a very small Pb–Pb bond character. The remaining six electrons would occupy the three nonbonding tangential 4p orbitals in the equatorial plane.

An equivalent molecular orbital description, which also corresponds to the valence bond description, can be arrived at by arranging the 4p (Se) and 6p (Pb) orbitals as follows: for a Se atom two 4p orbitals are directed toward the Pb atoms while the third 4p orbital is tangential, lies in the plane of the three Se atoms, and when filled, defines a lone pair on each Se; for a Pb atom, each of the three 6p orbitals lies along the edges of a $PbSe_3$ trigonal pyramid. In this scheme we consider the interaction of two 4p (Se) and all three 6p (Pb) atomic orbitals, where the third 4p orbital of Se is in the equatorial plane and is therefore nonbonding:

(21) Arsenault, J. J. I.; Dean, P. A. W. *Can. J. Chem.* **1983**, *61*, 1516.
(22) Dean, P. A. W. *Can. J. Chem.* **1982**, *60*, 2921.
(23) Huttner, G.; Weber, U.; Zsolnai, L. *Z. Naturforsch., B: Anorg. Chem., Org. Chem.* **1982**, *37B*, 707.
(24) Wells, A. F. *Structural Inorganic Chemistry*, 4th ed.; Oxford University Press: Oxford, England, 1975; Chapter 29, p 1013.
(25) Wade, K. *Adv. Inorg. Chem. Radiochem.* **1976**, *18*, 1.
(26) Desclaux, J. P. *At. Data Nucl. Data Tables* **1973**, *12*, 312.
(27) Drowart, J.; Honig, R. E. *J. Phys. Chem.* **1957**, *61*, 980.

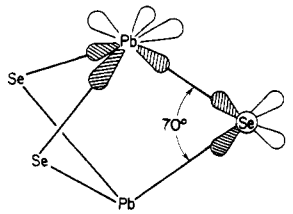

As the 4p and 6p atomic orbitals are now better directed with respect to each other, they interact more strongly. The result of this interaction is that the six strongly bonding molecular orbitals a_1', a_2'', e', and e'' are formed, resulting in a total of six bonding pairs of electrons for the $Pb_2Se_3^{2-}$ anion in accord with simple valence bond structure I. Formally, the above molecular orbital description of the bonding in $Pb_2Ch_3^{2-}$ anions does not allow for s-orbital involvement and is in qualitative agreement with the observed magnitudes of the relativistically corrected reduced coupling constants $(^1K_{Pb-Ch})_{RC}$ discussed earlier.

In the above molecular orbital description, the Pb atoms utilize the 6p orbitals in the bonding to the Se atoms. The use of the van der Waals distance of 4.0 Å between the Pb atoms in the $Pb_2Se_3^{2-}$ anion is therefore not appropriate, as that distance includes a contribution from 6p valence orbitals of lead (cf. ref 12). One should therefore use the size of the $6s^2$ core for lead as the "size" of the Pb core electrons ($5d^{10}6s^2$ included). One estimate of the size would be the ionic radius of Pb^{2+} (1.20 Å).[28] A better estimate of the size, as shown by Kammeyer and Whitman,[29] would be the univalent radius. Although the univalent radius of Pb^{2+} has not been reported, an upper limit may be established by using the ionic radius of Tl^+ (1.40 Å),[28] which, when doubled, is considerably under the Pb–Pb distance observed in $Pb_2Se_3^{2-}$. Presumably there is a repulsion between the two $6s^2$ cores in the anion, but the effect is small relative to the six filled bonding molecular orbitals. Furthermore, this repulsion is diminished by the polarization of the $6s^2$ cores away from each other due to the electron bond pairs of the $Pb_2Se_3^{2-}$ anion.

It would appear that the normal geometrical constraints of closest packing of selenium atoms in the equatorial belt and the inherent trigonal-pyramidal geometry of the $PbSe_3$ moieties of $Pb_2Se_3^{2-}$ give rise to the surprisingly short apical Pb–Pb distance and that the main features of the $Pb_2Se_3^{2-}$ anion structure are dictated by the stereochemical activity of the valence electron lone pair of each $PbSe_3$ kernel.

Relationship of $Pb_2Ch_3^{2-}$ to $Sb_2Se_4^{2-}$ and $Tl_2Ch_2^{2-}$. As noted earlier in this discussion, the NMR spectra of the $Pb_2Ch_3^{2-}$ anion containing selenium show an intense peak at −438 ppm in the ^{77}Se spectrum, which is assigned to the Se^{2-} anion. An intense ^{77}Se peak (−436 ppm) arising from Se^{2-} has also been reported for solutions resulting from the extraction of KTlCh alloys in en.[6] The latter alloys give rise to both trigonal-planar $TlCh_3^{3-}$ and butterfly-type $Tl_2Ch_2^{2-}$ species in solution. The ^{77}Se, ^{125}Te, and $^{203,205}Tl$ spectra of these extracts show the $Tl_2Ch_2^{2-}$ resonances are all significantly exchange-broadened at room temperature relative to those of the trigonal-planar series of $TlCh_3^{3-}$ anions. Our present work on the $Pb_2Ch_3^{2-}$ anion, recently published observations of the exchange behavior of $Tl_2Ch_2^{2-}$ species, and the recent X-ray structural determinations of *cis*- and *trans*-$Sb_2Se_4^{2-}$[30] suggest a close structural relationship exists among this series of chalcogenide anions.

Although all members of the series may be regarded as being derived from a M_2Ch_3-type trigonal bipyramid by formal removal or addition of Ch^{2-}, the observation of Se^{2-} in en solutions of the stable $Pb_2Ch_3^{2-}$ and $Tl_2Ch_2^{2-}$ anion series does not necessarily imply both species possess selenium-rich precursors such as $Pb_2Ch_4^{4-}$ and $Tl_2Ch_3^{4-}$, which undergo elimination of Ch^{2-} upon extraction into en. Rather, regardless of the penultimate origin of Se^{2-} in these solutions, it would appear that the high formal negative charges of the structurally related $Pb_2Ch_4^{4-}$ and $Tl_2Ch_3^{4-}$ anions, which have known isovalent $Sb_2Se_4^{2-}$ and $Pb_2Ch_3^{2-}$ analogues, are not effectively stabilized in solution with respect to the dinegative species $Tl_2Ch_2^{2-}$, $Pb_2Ch_3^{2-}$, and Se^{2-}. It might be anticipated that the −4 charges of $Pb_2Ch_4^{4-}$ and $Tl_2Ch_3^{4-}$ would be more effectively stabilized by the close naked cation–anion contact distances afforded in the solid state in the absence of a cryptating agent. Indeed, many examples of ternary main-group classical Zintl anions exist in the solid state in which the counteranion of the alkali-metal or alkaline-earth cation possesses a formal negative charge exceeding −4.[5]

In a previous discussion of KTlCh alloy extracts using 2,2,2-crypt in en,[6] equilibrium 4 was postulated in order to account for the trigonal-planar $TlCh_3^{3-}$ and the $Tl_2Ch_2^{2-}$ butterfly-type species.

$$2TlCh_3^{3-} \rightleftarrows Tl_2Ch_2^{2-} + 2Ch_2^{2-} \quad (4)$$

However, no evidence was found for Ch_2^{2-} although Se^{2-} was observed when selenium-containing alloys were extracted. The presence of Se^{2-} instead of Se_2^{2-} was explained by the known equilibrium (5).[31] No Se_3^{2-} was observed, however, and it was

$$Se_2^{2-} \rightleftarrows Se^{2-} + Se_3^{2-} \quad (5)$$

further suggested that, in the mixed Se/Te systems, mixed species such as $TeSe^{2-}$, Te_2Se^{2-}, and $TeSe_2^{2-}$ may be formed. Again, no NMR signals corresponding to any of those species could be observed in support of this postulate. The selective broadening of $Tl_2Ch_2^{2-}$ resonance lines in the ^{77}Se, ^{125}Te, and $^{203,205}Tl$ spectra of these species while the $TlCh_3^{3-}$ lines remain sharp also argues against equilibrium (4). Rather, the observation of Se^{2-} in the en extracts suggests equilibrium (6) is operative and that the

$$Tl_2Ch_2^{2-} + Ch^{2-} \rightleftarrows [Tl_2Ch_3^{4-}] \quad (6)$$

trigonal-bipyramidal $Tl_2Ch_3^{4-}$ anion could serve as a plausible intermediate in the chemical exchange of Ch^{2-}. In contrast, the ^{77}Se, ^{125}Te, and ^{207}Pb resonances of the series of mixed $Pb_2Ch_3^{2-}$ anions show no apparent exchange broadening in the presence of Se^{2-}. Chemical exchange with free Se^{2-} is presumed to be very slow on the NMR time scale and suggests that the $Pb_2Ch_3^{2-}$ trigonal-bipyramidal cage is inert. The number of M–Ch bonds and the formal charges of the metal are the same in $Pb_2Ch_3^{2-}$ and the hypothetical $Pb_2Ch_4^{4-}$(cis and/or trans) anion, whereas they increase in the proposed intermediate $Tl_2Ch_3^{4-}$. Furthermore, although the formal charges on the Pb atoms would not change, the formation of a species like $Pb_2Ch_4^{4-}$ from $Pb_2Ch_3^{2-}$ and Se^{2-} would inevitably involve M–Ch bond breaking and bond formation in contrast to the formation of $Tl_2Ch_3^{4-}$ from $Tl_2Ch_2^{2-}$ and Ch_2^{-} where bond formation is entailed and each Tl atom has available a vacant p orbital. The activation barrier for the formation of $Tl_2Ch_3^{4-}$ should therefore be much smaller. However, the high formal charge on the thallium atoms in $Tl_2Ch_3^{4-}$ (Tl^{2-}) presumably renders the anion thermodynamically unstable relative to $Tl_2Ch_2^{2-}$ and Ch^{2-}.

Experimental Section

Apparatus and Materials. A majority of the compounds used and prepared during the course of this work were air- and moisture-sensitive. Consequently, all manipulations were carried out under anhydrous conditions on glass vacuum lines or in a nitrogen-atmosphere drybox (Vacuum Atmospheres Model DLX). Drybox moisture and oxygen levels were routinely less than 0.01 ppm.

Potassium (MCB) was used as received, and freshly cut samples were handled only in the drybox. Lead, as shot (British Drug House, 99.9%), tellurium (Alfa Inorganics, 99.5%), and selenium (Alfa Inorganics, 99.9%) were used directly as obtained. 2,2,2-crypt (4,7,13,16,21,24-hexaoxa-1,10-diazabicyclo[8.8.8]hexacosane) was obtained from Merck and also used as received. Ethylenediamine (Fisher Scientific Co.) was dried over CaH_2 (MCB) for several weeks and then vacuum distilled onto and stored over fresh CaH_2 for at least 1 week prior to use.

Preparation of K–Pb–Ch Alloys. All alloys were prepared by fusion of the appropriate components in the required mole ratios in Pyrex vessels. This was accomplished in two stages. First, potassium and lead

(28) Reference 20, Chapter 13, p 518.
(29) Kammeyer, C. W.; Whitman, D. R. *J. Chem. Phys.* **1972**, *56*, 4419.
(30) Cordier, G.; Cook, R.; Schäfer, H. *Angew. Chem., Int. Ed. Engl.* **1980**, *19*, 324.
(31) Sharp, K. W.; Koehler, W. H. *Inorg. Chem.* **1977**, *16*, 2258.

were fused to give the binary alloy KPb. The required amounts of tellurium and/or selenium were then premixed and added to the binary alloy to give a K:Pb:Ch ratio of 1:1:1, where Se:Te was either $^1/_3$:$^2/_3$ or $^2/_3$:$^1/_3$ in the quaternary alloys. After complete reaction, the ternary/quaternary alloy was allowed to solidify and cool, transferred to the drybox, powdered, and stored in a glass vial until used. Even though the binary KPb alloy had formed, in no case was a homogeneous alloy obtained. Rather, a plug of lead metal amounting to ca. 50% of the initial lead was recovered, cleaned, and weighed. The stoichiometries of the final alloys were corrected accordingly. Alloys having the following compositions were prepared and subsequently extracted in ethylenediamine: $KPb_{0.56}Se_{0.33}Te_{0.67}$, $KPb_{0.54}Se_{0.67}Te_{0.33}$, $KPb_{0.49}Se$, and $KPb_{0.65}Te$.

Extraction of Alloy Phases. A stoichiometric amount of 2,2,2-crypt corresponding to the potassium metal was added and thoroughly mixed with powdered alloy in a glass ampule. The amount of alloy material used was adjusted such that the final amount of 2,2,2-crypt was approximately 0.2 g. After evacuation, approximately 10 mL of en was vacuum distilled onto the mixture and the tube and contents were allowed to warm to room temperature. Complete extraction of the alloys generally took place within 2–4 weeks. Samples were periodically agitated during the extraction period.

Preparation of NMR Samples. Following extraction of the alloy phases, the undissolved materials were allowed to settle before the clear solutions were decanted into precision 10-mm (o.d.) NMR tubes attached to the reaction vessels. The solutions were concentrated for NMR analysis through evaporation by cooling the portion of the reaction vessel containing the residual alloy in an ice-water bath. Slow static distillation of en from the NMR tube back onto the alloy was allowed to continue until a solvent column height suitable for NMR analysis was obtained or until a saturated solution had formed. After being cooled to 0 °C, the NMR tube and contents were isolated by flame sealing.

In general, anion concentrations ranged from about 0.10 *m* down to 0.065 *m* for extraction of the ternary alloys $KPb_{0.49}Se$ and $KPb_{0.65}Te$. For the extraction from the quaternary alloys $KPb_{0.56}Se_{0.33}Te_{0.67}$ and $KPb_{0.54}Se_{0.67}Te_{0.33}$ the concentration necessarily varied over a wider range because of the distribution of species depending on the alloy composition, with the concentration of the principal species in the range 0.065–0.10 *m*. The approximate distributions of the anions extracted from the quaternary alloys were estimated from relative NMR signal intensities and are as follows: for $KPb_{0.56}Se_{0.33}Te_{0.67}$, 30% $Pb_2Te_3^{2-}$, 50% $Pb_2SeTe_2^{2-}$, and 20% $Pb_2Se_2Te^{2-}$; for $KPb_{0.54}Se_{0.67}Te_{0.33}$, 5% $Pb_2Te_3^{2-}$, 15% $Pb_2SeTe_2^{2-}$, 40% $Pb_2Se_2Te^{2-}$, and 40% $Pb_2Se_3^{2-}$.

Multinuclear Magnetic Resonance Spectroscopy. All NMR spectra were recorded at an external applied field strength of 5.8719 T on a Bruker WM-250 pulse spectrometer equipped with a cryomagnet and consequently were run unlocked (field drift <0.1 Hz/h) at 24 °C. Spectra were obtained with use of 10-mm probes that were broad-banded over the frequency ranges 23–103 and 12–101 MHz. The observing frequencies were 47.704 MHz for ^{77}Se, 78.917 MHz for ^{125}Te, and 52.174 MHz for ^{207}Pb. Free-induction decays were typically accumulated in a 32K memory. Spectral width settings of 25 or 100 KHz were employed, yielding data point resolutions of 1.5 and 6.1 Hz and acquisition times of 0.656 and 0.164 s, respectively. No relaxation delay was applied. The number of free-induction decays accumulated varied with concentration and sensitivity of the nucleus under consideration, with 80 000–200 000 scans being typical for these dilute samples. Pulse widths corresponding to bulk magnetization tip angles, θ, of approximately 90° were 20 (^{77}Se), 20 (^{125}Te), and 25 μs (^{207}Pb). Line-broadening parameters used in exponential multiplication of the free-induction decays were 10–20 Hz.

Tetramethyllead was prepared by the standard literature method.[32] The sample was degassed and vacuum distilled into an 8 mm o.d. thin-walled glass NMR tube (cooled to −196 °C) and the frozen sample heat-sealed under dynamic vacuum. The 8-mm sample tube was centered, by means of Teflon shims, inside a 10-mm tube containing tetramethylsilane (Me_4Si) dissolved in $CDCl_3$ within its annular space, and the spectrometer was ^{2}H-locked on the solvent. The ^{1}H frequency of Me_4Si and the ^{207}Pb frequency of $(CH_3)_4Pb$ were then measured at 24 °C. The absolute frequency, Ξ, of ^{207}Pb in neat $(CH_3)_4Pb$ was then calculated to be 20.920 608 MHz (±10 Hz), assuming the protons in Me_4Si resonate at exactly 100 MHz. This value is in excellent agreement with the previously reported value of 20.920 597 MHz for 85% $(CH_3)_4Pb$ in toluene.[33]

The respective nuclei were referenced to neat samples of $(CH_3)_2Se$, $(CH_3)_2Te$ and $(CH_3)_4Pb$ at 24 °C. The chemical shift convention used is that a positive (negative) sign signifies a chemical shift to high (low) frequency of the reference compound.

X-ray Crystallography. The alloy $KPb_{0.49}Se$ was extracted in en in the presence of 2,2,2-crypt for 3 weeks, forming an orange solution. The supernatant solution was decanted from the alloy residue, and large orange crystals were grown by slow static distillation of the solvent at room temperature into a region of the apparatus that was a few degrees below room temperature. The mother liquor was decanted, and the crystals were dried under dynamic vacuum. The large well-formed crystals were cleaved into smaller fragments and sealed in 0.2–0.3-mm Lindemann capillaries in a dry (<1 ppm), nitrogen-filled glovebox equipped with a microscope. Further work was done on an Enraf-Nonius CAD4 diffractometer and a plate-shaped crystal bound by the form {010} and the faces (101), ($\bar{1}$0$\bar{1}$), (10$\bar{1}$), and ($\bar{1}$01), which were 0.0072, 0.0145, 0.0145, 0.0113, and 0.0113 cm from an origin within the crystal. Due to the long *b* axis, reflections from this crystal had to be well-centered before the correct orientation matrix could be obtained. Least-squares refinement of the diffracting position of 24 reflections ($6.7 < \theta < 14.4°$) gave the following crystal data.

Crystal Data: $C_{36}H_{72}K_2N_4O_{12}Pb_2Se_3$; fw = 1482.5; monoclinic, space group $P2_1/n$; a = 10.320 (4), b = 47.011 (11), c = 11.430 (4) Å; β = 90.25 (4)°; V = 5545 Å^3; D_{calcd} = 1.78 g cm^{-3} for Z = 4. Mo K$\bar{\alpha}$ radiation (λ = 0.710 69 Å, μ(Mo K$\bar{\alpha}$) = 82.6 cm^{-1}) was used.

X-ray Intensity Measurements. Estimated peak widths (in ω) during the reflection centering were 0.2–0.3° so that intensity data were collected by using ω–2θ scans over ω-scan ranges $(0.55 + 0.35 \tan \theta)°$. Scan rates conditional on information collected in prescans were chosen to give an $I/\sigma(I)$ ratio of 25 within a maximum scan time of 65 s. Backgrounds were obtained by extending the scan by 25% on either side of the peak and were measured for half the time taken to collect the peak. Three standard reflections collected after every 9500 s of exposure time showed only small (±3–4%) variation in intensities. A total of 10 457 reflections within the quadrants $h,k,\pm l$ with $2\theta < 50°$ were measured. Lorentz, polarization, and, at a later stage in the refinement, absorption corrections (program ABSCOR:[34] 10 × 6 × 10 grid; minimum T, 0.198; maximum T, 0.342) were applied to all the data. Exclusion of systematically absent and zero F_o data and averaging of 492 symmetry-equivalent data ($R_{merge}(F)$ = 0.064) gave a final data set of 8087 reflections.

Structure Solution. The structure was solved by using a combination of the Patterson function and direct methods to locate two Pb and two Se atoms in the anion. Least-squares and difference Fourier maps then located the missing non-hydrogen atoms and determined that the anion was $Pb_2Se_3^{2-}$. The peak height for the third Se atom was much lower than for the other two and resulted in a much higher temperature factor in the least-squares refinement. With all atoms isotropic the R_1 value was 0.2101. Substantial improvement in the residual was obtained by introducing anisotropic thermal parameters for Pb, Se, and K. Hydrogen atoms were then placed in calculated positions, absorption corrections were made, and a weighting scheme was introduced. Refinement then converged (maximum Δ/σ = 0.06) to the residuals R_1 = 0.1184 (R_2 = 0.1265) for 3956 data with $I > 3\sigma(I)$ (R_1 = 0.1256, R_2 = 0.1378 for the data uncorrected for absorption). High R factors are a feature of structures containing 2,2,2-crypt moieties, and in the present structure there is considerable anisotropy in the thermal parameters of the anion (notably Pb(1), Pb(2), and Se(3)) probably due to some slight static disorder of the anions. Refinement of the population parameters of the atoms in the anion gave values within 2σ of 1.0. Residual peaks up to 4.5 e Å^{-3} in height within 1.1 Å of Pb(1), Pb(2), and Se(3) are consistent with this proposal. Weights in the final cycles were given by $w = [\sigma^2(F) + 0.00262F^2]^{-1}$, and no systematic trends in the data were apparent after the use of this scheme.

All calculations were performed by using the Enraf-Nonius SDP package[34] and SHELX[35] on PDP 11/23 and Gould 9705 computers. Neutral-atom scattering factors in the analytical form were taken from ref 36 or were stored in the program.

Acknowledgment. We wish to thank the Natural Sciences and Engineering Research Council of Canada for providing operating grants (G.J.S.) and an equipment grant for the X-ray diffractometer (Chemistry Department, University of Toronto), and McMaster University for the award of a fellowship to M.B.

Registry No. en, 107-15-3; $KPb_{0.56}Se_{0.33}Te_{0.67}$, 106589-79-1; $KPb_{0.54}Se_{0.67}Te_{0.33}$, 106589-80-4; $KPb_{0.49}Se$, 106626-01-1; $KPb_{0.65}Te$,

(32) Singh, G. *J. Organomet. Chem.* **1968**, *11*, 133.
(33) Harris, R. K.; Kennedy, J. D.; McFarlane, W. In *NMR and the Periodic Table*; Harris, R. K., Mann, B. E., Eds.; Academic: London, 1978; Chapter 11, p 309.
(34) "Enraf-Nonius Structure Determination Package"; B. A. Frenz and Associates, Inc.: College Station, TX, 1981.
(35) Sheldrick, G. M. "SHELX Program for Crystal Structure Determination"; University of Cambridge: Cambridge, England, 1976.
(36) *International Tables for X-ray Crystallography*; Ibers, J. A., Hamilton, W. C., Eds.; Kynoch: Birmingham, England, 1974; Vol. 4.

106589-81-5; KPb, 106589-82-6; $Pb_2Te_3^{2-}$, 106589-74-6; $Pb_2SeTe_2^{2-}$, 106589-75-7; $Pb_2Se_2Te^{2-}$, 106589-76-8; (2,2,2-crypt-K^+)$_2Pb_2Se_3^{2-}$, 106589-78-0; $Pb_2Se_3^{2-}$, 106589-77-9; K, 7440-09-7; Pb, 7439-92-1; Te, 13494-80-9; Se, 7782-49-2; ^{207}Pb, 14119-29-0; ^{77}Se, 14681-72-2; ^{125}Te, 14390-73-9.

Supplementary Material Available: Tables of anisotropic thermal parameters and of bond distances and bond angles in the 2,2,2-crypt moieties and Figure 3 (stereopair), showing the packing of (2,2,2-crypt-K^+)$_2Pb_2Se_3^{2-}$ (4 pages); a listing of final structure factor amplitudes (20 pages). Ordering information is given on any current masthead page.

Contribution from the Department of Chemistry and Biochemistry, University of Windsor, Windsor, Ontario, Canada N9B 3P4

Toward Copper(II) Hemocyanin Models. 2.† Synthesis and Characterization of Binuclear Copper(II) Complexes of a Heptadentate Ligand

Hilde P. Berends and Douglas W. Stephan*

Received August 28, 1986

The preparation of the heptadentate ligand 2,6-bis[(bis(benzimidazolylmethyl)amino)methyl]-*p*-cresol (**4**) is described. The preparation of the copper complex formulated as $[Cu_2L(H_2O)_2][ClO_4]_3 \cdot 3H_2O$ (**5**) (L = anion of **4**) is given. The products of substitution reactions involving replacement of the coordinated water molecules of **5** with *N*-methylimidazole, pyridine, formate, acetate, pyrazolate, and azide gave a series of complexes **6**–**11**, respectively. UV–vis, electrochemistry, and EPR data are presented for these dicopper complexes. Variable-temperature magnetic susceptibility data are presented for complexes **5**, **7**, **9**, and **10**. The parent complex, **5**, is weakly ferromagnetic ($2J$ = 4.2 cm^{-1}); complex **7** is paramagnetic ($2J$ = 0.0 cm^{-1}), while **9** and **10** are weak antiferromagnets (**9**, $2J$ = −4.9 cm^{-1}; **10**, $2J$ = −77.8 cm^{-1}). The spectral and magnetic properties are discussed in the context of the known solid-state structure of **5**. The suitability of these complexes as models for the dicopper site of hemocyanin is discussed, and the implications for model design are considered.

Introduction

Inorganic chemists have contributed to the understanding of metalloproteins by the preparation and study of low molecular weight compounds designed to mimic both the structure and chemistry of metal ions in biology.[1] This "bioinorganic" or "biomimetic" approach has recently been applied to a number of copper-containing proteins.[2] One such system is the dicopper protein hemocyanin (Hc).[3-15] The function of this "type 3" copper enzyme is to bind and transport molecular oxygen in the hemolymph of molluscs and arthropods. The nature of the copper site is not entirely clear; however, EXAFS,[16,17] resonance Raman,[18] and other physicochemical studies[19-21] suggest that each copper ion in the oxy form of the protein is pentacoordinate. The coordination sphere is thought to include two or three imidazole (histidine) ligands, an endogenous oxygen atom bridge, and a peroxide moiety as in **1**. The source of the bridging oxygen is

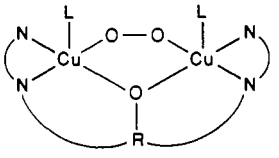

1

the subject of considerable speculation. Initially, it was postulated to be a phenolate oxygen from a tyrosine residue. However, recent crystallographic studies on deoxy-Hc call into question these earlier speculations and suggest that phenolate is not the bridging group.[22] The Cu–Cu separation is 3.67 Å.[16,17] In oxy-Hc, the bridging ligands presumably mediate antiferromagnetic coupling between the copper atoms, resulting in the observed diamagnetism at room temperature. An EPR-detectable met form of Hc (Cu(II)–Cu(II)) is also known.[2] Early approaches to modeling this dicopper center utilized Schiff bases or other unsaturated ligands.[23] Recently, attention has focused on complexes that are designed to better mimic the biological environment of the copper ions in hemocyanin.[3-15] To this end, we have prepared the ligand 2,6-bis-[(bis(benzimidazolylmethyl)amino)methyl]-*p*-cresol (**4**).[14]

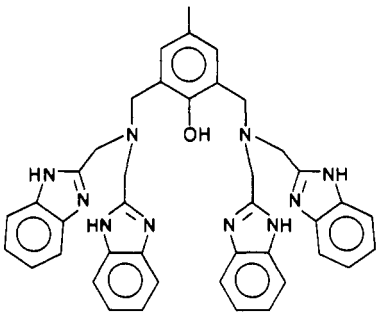

4

In this paper, we describe the synthesis of **4** and a series of derivatives of **4** containing a variety of exogenous ligands. The

* To whom correspondence should be addressed.
† Part 1 to be considered ref 14.

(1) Holm, R. H.; Ibers, J. A. *Science* (*Washington, D.C.* **1980**, *209*, 223.
(2) Spiro, T., Ed. *Copper Proteins, Metal Ions in Biology*; 1981; Vol. 3.
(3) Sorrell, T. N.; O'Connor, C. J.; Anderson, O. P.; Reibenspies, J. H. *J. Am. Chem. Soc.* **1985**, *107*, 4199.
(4) Sorrell, T. N.; Jameson, D. L.; O'Connor, C. J. *Inorg. Chem.* **1984**, *23*, 190.
(5) McKee, V.; Zvagulis, M.; Reed, C. A. *Inorg. Chem.* **1985**, *24*, 2914.
(6) McKee, V.; Zvagulis, M.; Dagdigian, J. V.; Patch, M. G.; Reed, C. A. *J. Am. Chem. Soc.* **1984**, *106*, 4765.
(7) McKee, V.; Dagdigian, J. V.; Bau, R.; Reed, C. A. *J. Am. Chem. Soc.* **1981**, *103*, 7000.
(8) Karlin, K. D.; Cohen, B. I. *Inorg. Chim. Acta* **1985**, *107*, L17.
(9) Karlin, K. D.; Shi, J.; Hayes, J. C.; McKown, J. W.; Hutchinson, J. P.; Zubieta, J. *Inorg. Chim. Acta* **1984**, *91*, L3.
(10) Suzuki, M.; Uehara, A. *Inorg. Chim. Acta* **1984**, *87*, L29.
(11) Suzuki, M.; Kanatomi, H.; Murase, I. *Bull. Chem. Soc. Jpn.* **1984**, *57*, 36.
(12) Karlin, K. D.; Dalstrom, P. L.; Cozzette, S. N.; Scensny, P. M.; Zubieta, J. *J. Chem. Soc., Chem. Commun.* **1981**, 881.
(13) Karlin, K. D.; Haka, M. S.; Cruse, R. W.; Gultneh, Y. *J. Am. Chem. Soc.* **1985**, *107*, 5828.
(14) Berends, H. P.; Stephan, D. W. *Inorg. Chim. Acta* **1985**, *99*, L53.
(15) Nishida, Y.; Shimo, H.; Machara, H.; Kida, S. *J. Chem. Soc., Dalton Trans.* **1985**, 1945.
(16) Brown, J. M.; Powers, L.; Kincaid, B.; Larrabee, J. A.; Spiro, T. G. *J. Am. Chem. Soc.* **1980**, *102*, 4210.
(17) Woolerty, G. L.; Powers, L.; Winkler, M.; Solomon, E. I.; Spiro, T. G. *J. Am. Chem. Soc.* **1984**, *106*, 86.
(18) Larrabee, J. A.; Spiro, T. G. *J. Am. Chem. Soc.* **1980**, *102*, 4217.

0020-1669/87/1326-0749$01.50/0